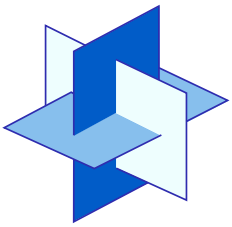

DFG-Research Center MATHEON
Mathematics for key technologies

Optimal PDE Control Using COMSOL Multiphysics[1]

Ira Neitzel[2]
Technische Universität Berlin, Sekr. MA 4-5
Straße des 17. Juni 136
D-10623 Berlin, Germany
neitzel@math.tu-berlin.de

Uwe Prüfert[3]
Technische Universität Berlin, Sekr. MA 4-5
Straße des 17. Juni 136
D-10623 Berlin, Germany
pruefert@math.tu-berlin.de

Thomas Slawig[4]
Christian-Albrechts-Universität zu Kiel, Technische Fakultät
Christian-Albrechts-Platz 4
D-24118 Kiel, Germany
ts@informatik.uni-kiel.de

[1]To appear on the proceedings CD of the 2008 COMSOL User Conference, Hannover (Germany)
[2]Research supported by DFG SPP 1253
[3]Resaerch supported by the DFG Research Center MATHEON
[4]Research supported by the Excellence Cluster *The Future Ocean, Algorithmic Optimal Control – Oceanic CO_2-Uptake* and DFG SPP 1253

Optimal PDE Control Using COMSOL Multiphysics

Ira Neitzel, Uwe Prüfert and Thomas Slawig

Abstract: We study an optimal control problem (OCP) subject to a PDE of elliptic type as well as state constraints. The resulting optimality system contains two PDEs, one algebraic equation and the so called complementary slackness conditions, i.e. dual products between function spaces. At this point different regularization techniques come into use. In this paper we introduce a Barrier method as one possible way to regularize state constraints, which leads to an easily implementable path-following algorithm.

To illustrate this method, we solve first a constructed problem with known solution. Here, we can verify the rate of convergence of the path-following method. Second, a simplified hyperthermia problem in 3D is solved by using COMSOL Multiphysics.

Keywords: Optimal control, bio heat transfer, Barrier method.

1. Introduction

Optimal PDE control is a challenging field of recent research, with growing impact in medicine, engineering, constructing etc. The following optimal control problem is topic of project A1 within MATHEON.

Regional hyperthermia is a cancer therapy aiming at heating large, deeply seated tumors in order to make them more susceptible to an accompanying radio or chemo therapy. The heat is introduced into the human body by absorption of radio-frequency electromagnetic waves originating from a phased array applicator. Figure 1 shows a model of a microwave applicator.

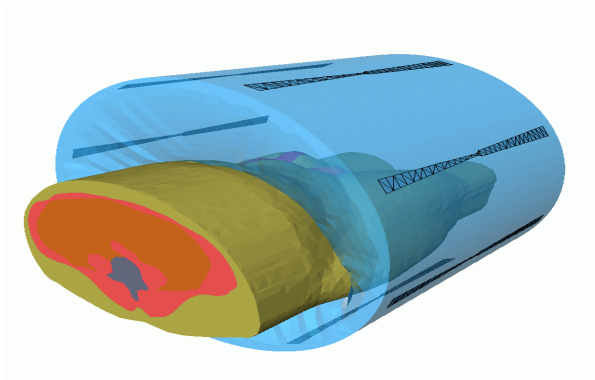

Figure 1. Virtual 3D model of a microwave applicator with a part of a virtual patient. Picture courtesy of Zuse Institute Berlin.

From the modelers point of view, the problem reads: The tumor should be heated up to the therapeutic temperature, but the temperature in the healthy tissue should not be higher than a compatible temperature. The temperature distribution is driven by

the bio-heat-transfer equation (BHTE), which is of elliptic type. Our aim is to optimize a source for the BHTE that creates an optimal temperature profile in the human body. The control parameters of the real word problem are actual the amplitudes and phase delays of the antennas of the microwave applicator. The hyperthermia problem is a typical task for optimal control.

In general, two antithetic strategies of optimal control are known. First, one can discretize the problem and optimize it by using e.g. a nonlinear programming software. The other way is to find optimality conditions for the continuous problem. These conditions are systems of PDEs and algebraic and/or integral equations. Here, COMSOL Multiphysics comes into action.

2. Problem definition

To model the regional hyperthermia, we consider the optimal control problem (HYPER):

$$\min \frac{1}{2}\int_\Omega (T - T_d)^2 + \kappa u^2 dx$$

subject to the elliptic PDE

$$\begin{aligned} -\nabla \cdot (A\nabla T) + a_0(T - T_{37}) &= u \text{ in } \Omega \\ \vec{n} \cdot (A\nabla T) + \alpha_0(T - T_b) &= 0 \text{ on } \Gamma. \end{aligned} \tag{1}$$

Optionally, let point-wise state constraints be given:

$$\begin{aligned} T_{therapeutic} \quad \leq \quad & T \qquad \text{in } \Omega_{tumor}. \\ T \leq \quad & T_{healthy} \text{ in } \Omega \backslash \Omega_{tumor} \end{aligned}$$

The domain $\Omega \subset \mathbb{R}^3$ is the human body (or a part of it), Γ is the boundary of Ω, i.e. the skin, or – if we consider only a part of the body – an intersection.

The temperature T is called the state and has to be from the space of almost everywhere bounded functions $L^\infty(\Omega)$. A solution of (1) belongs to this space for space dimensions $N \leq 3$.

3. Theoretical preparations

In this section we will use the usual "mathematical" names for the state, i.e. we will write y instead of T. Later, when we consider the problem of optimal temperature control again, we will use the "physical" notation.

3.1. **The state constrained problem.**

We consider the problem (OCP)

$$\min \frac{1}{2}\int_\Omega (y - y_d)^2 + \kappa u^2 \, dx$$

subject to the PDE (written as operator equation)

$$\mathbf{A}y \;=\; \mathbf{B}u \tag{2}$$

and to the state constraints

$$y_a \leq y \leq y_b \text{ a.e. in } \Omega.$$

Here, the operator equation is the weak formulation of a PDE in divergence form:

$$\int_\Omega \nabla v A \nabla y + a_0 y v + \int_\Gamma \alpha_0 y v \, ds = \int_\Omega uv \, dx + \int_\Gamma gv \, ds \quad \forall\, v \in H^1(\Omega), \tag{3}$$

cf. e.g. [2]. Let Y be a function space, e.g. the space $H^1(\Omega) \cap C(\bar{\Omega})$ or $L^2(\Omega)$.

We say a function $y \in Y$ is admissible, iff it fulfills the inequality constraints. The set of all admissible states is called the admissible set Y_{ad}.

The objective functional

$$J(y,u) := \frac{1}{2} \int_\Omega (y - y_d)^2 + \kappa u^2 \, dx \tag{4}$$

has some important properties:

- it is continuous for all $(y,u) \in (H^1(\Omega) \cap C(\bar{\Omega})) \subset L^2(\Omega) \times L^2(\Omega) \to \mathbb{R}$,
- it is strongly convex, i.e. $J(\theta(y_1,u_1) + (1-\theta)(y_2,u_2)) < \theta J(y_1,u_1) + (1-\theta)J(y_2,u_2)$ for all $\theta \in (0,1)$, and
- it is coercive, i.e. $\|J(y,u)\| \to \infty$ if $\|(y,u)\| \to \infty$.

The next theorem provides the existence of an unique solution of (OCP).

Theorem 3.1. *If Y_{ad} is convex and has non-empty interior, the functional J is continuous, strongly convex, and coercive, then the problem*

$$\min_{y \in Y_{ad}} J(y,u)$$

subject to

$$\mathbf{A}y = \mathbf{B}u$$

has a unique solution $(y^*, u^*) \in Y_{ad} \times L^2(\Omega)$.

We can show that our problem fulfill the assumptions of the last theorem.

Theorem 3.2. *Let $(y,u)^*$ be the solution of the Problem (OCP). Then, there are Lagrange multipliers η_a and η_b from the space of regular Borel measures and an adjoint state p such that the pair (y^*, u^*) together with p and η_a, η_b fulfills*

- *the adjoint equation*

$$\mathbf{A}^* p = \int_\Omega (y^* - y_d)\, v \, dx - \int_\Omega v \, d\eta_a + \int_\Omega v \, d\eta_b \, \forall\, v \in H^1(\Omega),$$

- *the gradient equation*

$$\mathbf{B}^* p + \kappa \int_\Omega u^* v \, dx = 0 \; \forall\, v \in L^2(\Omega),$$

- *the state equation*

$$\mathbf{A}y = \mathbf{B}u,$$

and

- *the complementary slackness conditions (CSC)*

$$\begin{aligned} \int_{\bar{\Omega}} (y^* - y_a)\, d\eta_a &= 0 \\ \int_{\bar{\Omega}} (y_b - y^*)\, d\eta_b &= 0 \\ \eta_a, \eta_b, (y^* - y_a), (y_b - y^*) &\geq 0 \quad \textit{in } \Omega. \end{aligned}$$

By setting $\int_\Omega uv\, dx = -\frac{1}{\kappa}\mathbf{B}^* p$ we can eliminate the gradient equation. The right-hand side of the adjoint equation is measure valued. Consequently, the adjoint state is less regular than the state. Note, that in the CSC the measures to the integrals are η_a and η_b resp. That is not the same as e.g. $\int_\Omega (y^* - y)\eta_a\, dx$. The condition $\eta_a, \eta_b \geq 0$ means that η_a,η_b are positive measures rather than a point-wise evaluation.

To implement the CSC we regularize it. Here, some different techniques are in use. We mentioned e.g. the Moreau-Yosida regularization, which makes it necessary to implement a PDE with a smoothed version of the maximum function on the right-hand-side in COMSOL Multiphysics. Examples and more references are given in [1].

3.2. **The Barrier Method.** Another way to solve OCPs with point-wise state constraints are Barrier methods. Barrier methods eliminate the constraint(s) by adding a so called barrier functional, e.g.

$$\begin{aligned} b(y;\mu) = -\mu \int_\Omega &\ln(y - y_a) \\ &+ \ln(y_b - y)\, dx + \chi_{Y_{ad}}(y), \end{aligned} \tag{5}$$

to the objective function, which results in optimality systems with nonlinear couplings between the PDEs. An algorithm to solve this optimality system can now easily be implemented in COMSOL.

In (5), χ is the indicator function defined by

$$\chi_{Y_{ad}}(y) = \begin{cases} 0 & \text{if } y \in Y_{ad} \\ \infty & \text{if } y \notin Y_{ad} \end{cases}.$$

The Barrier functional has some remarkable properties:

- $b(y) \leq \infty$ if $y \in Y_{ad}$ and $\text{meas}\{x \in \Omega \,|\, y_a(x) = y(x) \text{ or } y_b(x) = y(x)\} = 0$,
- $b(y) = \infty$ if $y \notin Y_{ad}$,.
- $b(y) \to \infty$ if $y \to \partial Y_{ad}$.
- if $y \in Y_{ad} \backslash \partial Y_{ad}$ (i.e. the interior of Y_{ad}) then $b(y)$ is directional differentiable in all directions $h \in L^2(\Omega)$ with

$$b(y)'h = \int_\Omega \left(\frac{\mu}{y_b - y} - \frac{\mu}{y - y_a} \right) h\, dx.$$

We consider now the problem (IP):

$$\begin{aligned} \min \int_\Omega &(y - y_d)^2 + \kappa u^2 \\ &- \mu \ln(y - y_a) + \ln(y_b - y)\, dx + \chi_{Y_{ad}}(y) \end{aligned}$$

subject to the PDE

$$\mathbf{A}y = \mathbf{B}u.$$

Note that this problem does not have any inequality constraints.

Barrier (or Interior-Point) methods are extensively investigated in some recent papers as e.g. [3], [4], such that we will summarize here the main results without proof.

Theorem 3.3. *(Existence of the Central Path) The Problem (IP) has for every $\mu > 0$ a unique solution $(y,u)_\mu$. The state y_μ holds $y_\mu = y_a$ or $y_\mu = y_b$ only on subsets of Ω with measure zero.*

Theorem 3.4. *(Convergence of the Central Path) Let $(y,u)^*$ be the unique minimizer of Problem (OCP). Then for for every $\mu > 0$ the error estimate*

$$\|(y,u)_\mu - (y,u)^*\| \leq c\sqrt{\mu}$$

holds for a $c > 0$.

Theorem 3.5. *(Optimality system) Let (y_μ, u_μ) be the unique minimizer of Problem (IP). Assume that y_μ holds $y_a(x) < y(x) < y_b(x)$ almost everywhere in Ω. Then there is an adjoint state p_μ such that (y_μ, u_μ) together with p_μ fulfill*

- *the adjoint equation*

$$\begin{aligned}\mathbf{A}^* p_\mu = &\int_\Omega (y_\mu - y_d)\, v\, dx \\ &- \int_\Omega \frac{\mu}{y_\mu - y_a} v\, dx + \int_\Omega \frac{\mu}{y_b - y_\mu} v\, dx, \\ &\qquad \forall\, v \in H^1(\Omega)\end{aligned}$$

- *the gradient equation*

$$\mathbf{B}^* p + \kappa \int_\Omega u_\mu v\, dx = 0 \;\forall\, v \in L^2(\Omega),$$

  and
- *the state equation*

$$\mathbf{A}y_\mu - \mathbf{B}u_\mu = 0.$$

One difference to Theorem 3.2 is that here no Lagrange multipliers appear, instead we have two integrals over rational functions. In view of later programming in COMSOL, we reformulate the optimality system in terms of Lagrange multipliers. By the setting $(\eta_a)_\mu = \frac{\mu}{y_\mu - y_a}$ and $(\eta_b)_\mu = \frac{\mu}{y_b - y_\mu}$ we can introduce approximations of the original Lagrange multipliers. These approximations are at least from $L^1(\Omega)$, which is a better space than the space of Borel measures. We insert $(\eta_a)_\mu$ and $(\eta_b)_\mu$ in the adjoint equation. To make this formulation valid, the weak complementary slackness condition

$$\begin{aligned}\int_\Omega (y_\mu - y_a)\,(\eta_a)_\mu\, dx &= \mu \\ \int_\Omega (y_b - y_\mu)\,(\eta_b)_\mu\, dx &= \mu\end{aligned} \tag{6}$$

together with the claim

$$(y_\mu - y_a), (y_b - y), (\eta_a)_\mu, (\eta_b)_\mu \geq 0 \tag{7}$$

has to be fulfilled. From the Gradient equation we get again

$$-\mathbf{B}u = -\int_\Omega uv\,dx = \frac{1}{\kappa}\mathbf{B}^* p.$$

Note, that this weak CSC is more regular than the original one from Theorem 3.2. Further, we remark that by changing the role of u and v in (3) the operators $\mathbf{A}$ and $\mathbf{A}^*$ as well as $\mathbf{B}$ and $\mathbf{B}^*$ have the same integral representation.

We implement the conditions (6) and (7) by the so called (smoothed) Fischer-Burmeister function

$$\Phi_{FB}(y, y_c, \eta_c; \mu) := \\ (y - y_c) + \eta_c - \sqrt{(y - y_c)^2 + \eta_c^2 + 2\mu}.$$

It is easy to show that $\Phi_{FB}(y, y_c, \eta_c; \mu) = 0$ is equivalent to $(y - y_c)\eta_c = \mu$ and $(y - y_c), \eta_c \geq 0$. The Fischer-Burmeister function is a so called nonlinear complementary function (NCP).

By

$$H(y, p, \eta_a, \eta_b) := \begin{pmatrix} \mathbf{A}^* p - \mathbf{B}(y - y_d \\ \qquad -\eta_a + \eta_b) \\ \mathbf{A}y + \frac{1}{\kappa}\mathbf{B}^* p \\ \Phi_{FB}(y, y_a, \eta_a; \mu) \\ \Phi_{FB}(y_b, y, \eta_b; \mu) \end{pmatrix}, \tag{8}$$

we can sample the optimality system into a function H. The mapping $\mu \mapsto (y, p, \eta_a, \eta_b)_\mu$ is called the Central Path. One can show, cf. e.g. [4], that this mapping is (Lipschitz) continuous.

3.3. **Path-following algorithm.** A conceptual algorithm in function spaces for our Barrier method is given by the following lines:

Algorithm 1 Barrier Method

Choose $0 < \sigma < 1$, $0 < eps$,
a initial solution $(y, p, \eta_a, \eta_b)^0$ such that
$y_a < y^0 \leq y_b$. Choose $\mu_0 > 0$. Set $k = 0$.
while $\mu_k > eps$
{
  $\mu_{k+1} = \sigma\mu_k$
  $d^{k+1} = -\partial H((y, p, \eta_a\eta_b)^k; \mu_{k+1})^{-1} H(y, p, \eta_a, \eta_b)^k; \mu_{k+1})$
  $(y, p, \eta_a, \eta_b)^{k+1} = (y, p, \eta_a, \eta_b)^k + d^{k+1}$
  $k = k + 1$
}

Within the while loop we take only one Newton step from $(y, p, \eta_a, \eta_b)^k$ in direction $\partial H(y, p, \eta_a, \eta_b)^k$. By this, we construct a polygonal (in function space) that approximates the Central Path. In Figure 2 we sketch this method.

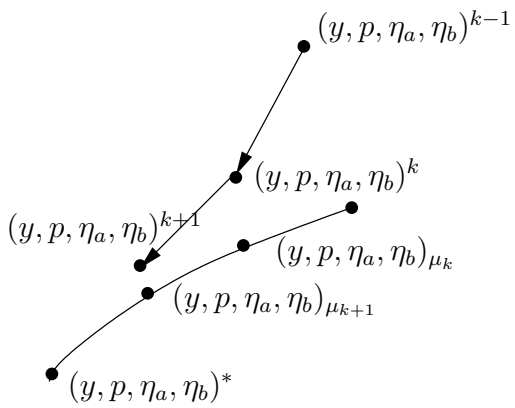

FIGURE 2. Sketch of Algorithm 1.

4. Applications

4.1. **An academical example.** For testing our algorithm, we first consider the following simple example (cf. e.g. [3]):

$$\min \frac{1}{2}\int_\Omega (y-y_d)^2 + u^2 dx,$$

such that the pair (y,u) fulfills the elliptic PDE

$$\begin{aligned} -\Delta y + y &= u \quad \text{in } \Omega \\ \vec{n}\cdot(\nabla y) &= 0 \quad \text{on } \Gamma, \end{aligned}$$

and the point-wise state constraint

$$y_a \leq y \quad \text{a.e. in } \Omega.$$

We set

$$\begin{aligned} &y_d(x_1,x_2) \\ &\quad = 4 - \max\{-20((x_1-0.5)^2 \\ &\qquad + (x_2-0.5)^2) + 1, 0\}, \\ &y_a(x_1,x_2) \\ &\quad = \min\{-20((x_1-0.5)^2 \\ &\qquad + (x_2-0.5)^2) + 3, 2\}. \end{aligned}$$

It can easily be shown that $u^* = 2$, $p = -2$, $y^* = 2$, together with

$$\eta_a = \max\left\{-20\left((x_1-0.5)^2 + (x_2-0.5)^2\right) + 1, 0\right\}$$

fulfill the optimality system given by Theorem 3.2.

Using (8), we can now easily implement our path-following algorithm in COMSOL. We use the general form of a PDE. First we define the function H:

```
fem.equ.ga = { { {'-yx1' '-yx2'}
                 {'-px1' '-px2'}
                 {'0' '0'} } };
fem.equ.f = { {'-y-1/kappa*p'...
 '-p+y-y_d(x1,x2)-eta'...
```

```
 'eta+(y-y_c(x1,x2)-sqrt(eta^2...
  +(y-y_c(x1,x2))^2)-2*mu)'} };
```

To get an initial solution for Algorithm 1, we solve the problem first for μ_0 with a high number (e.g. 50) of possible Newton steps. Next, we compute an adaptively refined mesh by using `adaption`, where the maximal number of Newton steps is set to 50.

The heart of the program, the path-following loop, can be simply implemented by

```
mu=1e-1;
while mu>1e-8,
    mu = mu*0.85;
    fem.const{4} =  num2str(mu);
    fem.xmesh = meshextend(fem);
    fem  = femnlin(fem,...
            'init',fem.sol,...
            'out','fem',...
            'Damping','off',...
            'Maxiter',1);
end
```

Note, that we now set the number of Newton steps to one and turn off the damping of the Newton method. This implements exactly the method as described in Algorithm 1. `Femnlin` returns the warning `Returned solution has not converged` which we can ignore: The convergence of the IP-path-following algorithm is ensured by the choice of the parameter σ. In our program we set $\sigma = 0.85$. Further, we chose $eps = 10^{-8}$.

The following figures show the computed solutions $\tilde{y} = y^{\mu_{eps}}$, $\tilde{p} = p^{\mu_{eps}}$ and the Lagrange multiplier $\tilde{\eta}_a = \eta_a^{\mu_{eps}}$.

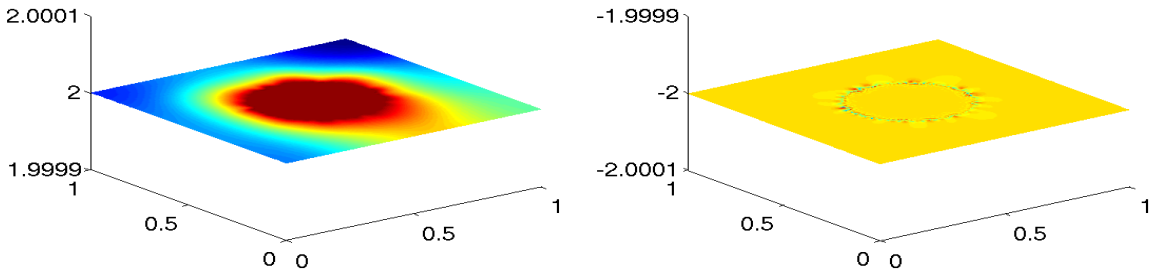

(a) (b)

FIGURE 3. Numerically computed optimal state $\tilde{y}$ and adjoint state $\tilde{p}$.

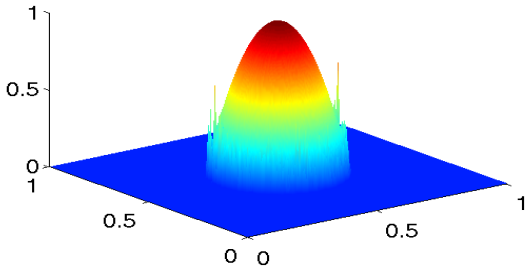

FIGURE 4. Lagrange Multiplier $\tilde{\eta}_a$.

Note, that y^μ, p^μ, and η^μ refer to iterates of Algorithm 1 while y_μ, p_μ, and η_μ are points on the central path. Note further, the scale of the z-axis in Figure 3 is 10^{-4}. In Figure 4 some peaks appear on the border of the active set, i.e. the subset of all $x \in \Omega$ where $\eta_a > 0$. This causes the rather large errors of the Lagrange multiplier, cf. Table 1. One can find the influence of these peaks also in the adjoint state p_μ, cf. Figure 3 (b). Here, by $\mu \to 0$ the NCP-function becomes non-differentiable in points where $\eta_a = 0$ and $(y - y_a) = 0$.

Having exact optimal solutions at hand, we are able to determine errors between e.g. y^μ and y^*. Table 1 shows the convergence of y^μ, p^μ, and $(\eta_c)^\mu$.

μ	$\|\tilde{y} - y^*\|_{L^2}$	$\|\tilde{p} - p\|_{L^2}$	$\|\tilde{\eta}_c - \eta_a\|_{L^2}$
10^{-2}	$2.09 \cdot 10^{-2}$	$2.09 \cdot 10^{-2}$	$1.28 \cdot 10^{-1}$
10^{-3}	$2.12 \cdot 10^{-3}$	$2.12 \cdot 10^{-3}$	$5.62 \cdot 10^{-2}$
10^{-4}	$2.17 \cdot 10^{-4}$	$2.10 \cdot 10^{-4}$	$2.06 \cdot 10^{-2}$
10^{-5}	$2.23 \cdot 10^{-5}$	$2.23 \cdot 10^{-5}$	$9.036 \cdot 10^{-3}$
10^{-6}	$2.29 \cdot 10^{-6}$	$2.29 \cdot 10^{-6}$	$8.34 \cdot 10^{-3}$
10^{-7}	$1.99 \cdot 10^{-7}$	$2.11 \cdot 10^{-7}$	$1.18 \cdot 10^{-2}$
10^{-8}	$2.03 \cdot 10^{-8}$	$6.94 \cdot 10^{-8}$	$1.22 \cdot 10^{-2}$

TABLE 1. Results to Example 1.

In Figure 6, the linear convergence in state y^μ and adjoint state p^μ (and by $u^\mu = \frac{1}{\kappa} p^\mu$ also in u^μ) is visible.

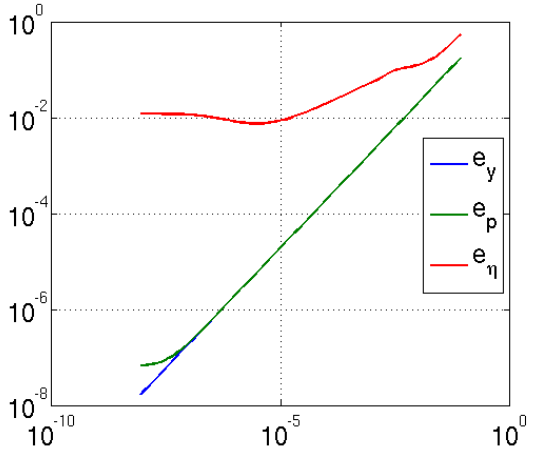

FIGURE 5. Errors $\|y^\mu - y^*\|_{L^2(\Omega)}$, $\|p^\mu - p^*\|_{L^2(\Omega)}$ and $\|(\eta_a)^\mu - \eta_a\|_{L^2(\Omega)}$. Both axis are scaled logarithmically.

The error in the Lagrange multiplier stagnates for $\mu < 10^{-5}$. This is caused by the discretization error and the peaks resulting from the numerical destabilization of the method for very small μ. This is not a drawback of this method, but one task when using regularizations is to find a balance between disturbing the problem and the improvement for the behavior of the method by the regularization. In this example the path following should be stopped at $eps = 10^{-5}$.

4.2. **The optimal control of the thermoregularization.** In this section we return to the problem (HYPER). We simplify our patient in the following way: We consider only the part of the body (e.g. the leg or a part of it) where the tumor is situated. The cut offs of the rest of the body are modeled by do-nothing boundary conditions. We identify the tumor as an ellipsoid inside the muscle tissue. In the different kinds of tissue we have the following diffusion and perfusion coefficients.

tissue	a_{ii}	a_0
muscle	0.5	3.8
fat	0.2	1.6
bone	0.3	0.05
tumor	0.2	0.5

TABLE 2. Thermal conductivity and perfusion coefficients.

The desired temperature and the constraints are defined by

$$T_d = \begin{cases} 45 & x \in \Omega_{tumor} \\ \text{any} & x \in \Omega \backslash \Omega_{tumor} \end{cases},$$

$$T_{therapeutical} = \begin{cases} 45 & x \in \Omega_{tumor} \\ 36 & x \in \Omega \backslash \Omega_{tumor} \end{cases},$$

and

$$T_{healthy} = \begin{cases} 48 & x \in \Omega_{tumor} \\ 41 & x \in \Omega \backslash \Omega_{tumor} \end{cases}.$$

The lower bound T_a guaranties the effect of the hyperthermia, and T_b is a safety bound to protect the patient. Note, that T_d is defined only in Ω_{tumor}. Further, we set the outside temperature $T_b = 36$ and $\alpha_0 = 1.2$.

By using our algorithm we obtain the optimal temperature provided in Figure 7 (a).

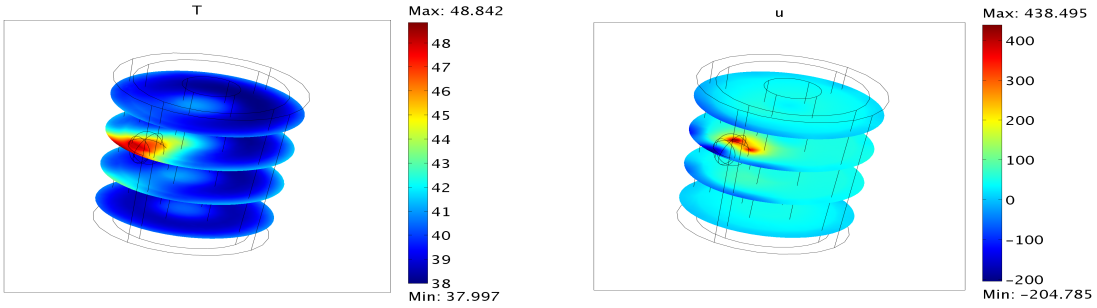

(a) (b)

FIGURE 6. Optimal temperature $T^{\mu_{eps}}$ and Optimal control $u^{\mu_{eps}}$.

The dark blue colored region is muscle tissue with strong blood perfusion. Note the relatively hot region in the center. This is caused by the good heat conduction by a coincidental lack of perfusion inside the bone. Figure 7 (b) presents the optimal heat distribution. Blue colors mark regions where the patient should be cooled.

5. Conclusion

Having access to the optimality system in PDE form, COMSOL Multiphysics provides by its capability to solve coupled non-linear systems of PDEs an easily implementable way to solve optimal control problems. An algorithm based on barrier methods was successfully tested on an academical problem with known solution as well as on the 3D hyperthermia model problem. Applicability of this method to other realistic problems has to be decided depending on the complexity of the problem.

References

[1] I. Neitzel, U. Prüfert, and T. Slawig. Strategies for time-dependent PDE control with inequality constraints using an integrated modeling and simulation environment. *Numerical Algorithms*, 2008.

[2] U. Prüfert and A. Schiela. The minimization of an L^∞-functional subject to an elliptic PDE and state constraints. ZIB-Report, Konrad-Zuse-Zentrum für Informationstechnik Berlin, 2008.

[3] U. Prüfert, F. Tröltzsch, and M. Weiser. The convergence of an interior point method for an elliptic control problem with mixed control-state constraints. *Comput. Optim. Appl.*, 39(2):183–218, 2008.

[4] A. Schiela. An extended mathematical framework for barrier methods in function space. ZIB-Report 08-07, Konrad-Zuse-Zentrum für Informationstechnik Berlin, 2008.